

## SCOUR PROPERTIES DOWNSTREAM FREE HYDRAULIC JUMPS ON CORRUGATED BEDS

خصائص النحر خلف القفزات الهيدروليكية الحرة علي القيعان المتموجة

Zidan, A.R., El-Alfy, K.S., Abdalla, M.G., and Ibrahiem, M.I.

Irrigation and Hydraulics Dept., Faculty of Engineering, El-Mansoura University

### خلاصة:

يهدف هذا البحث إلى دراسة تأثير خمسة نماذج من القيعان المتموجة وهي عبارة عن: أنصاف دوائر، أشباه منحرفات، أشباه منحرفات بينها مسافات بيئية، مثلثية، ومثلثية بينها مسافات بيئية (إضافة إلى القاع الأملس) على خصائص النحر خلف القفزات الهيدروليكية الحرة المتولدة. هذه القيعان تعمل على توليد دوامات اضطرابية وزيادة إجهادات القص مما يزيد من خشونة قاع المجري المائي. يصاحب ذلك تقليل في كل من العمق المتعاقب للقفزة الهيدروليكية وطولها مما قد يؤدي إلى تحريك القفزة الهيدروليكية بالقرب من بوابة الحجز بعيدا عن القاع المتحرك وهذا بدوره يقلل من عمق وطول النحر المتولد. تمت الدراسة المعملية بإجراء 285 تجربة باستخدام ثلاثة أنواع من عينات الرمل المختلفة (عينة من الرمل الناعم ذات قطر حبيبات متوسط 0.167 مم، عينة من الرمل المتوسط ذات قطر حبيبات متوسط 0.365 مم وعينة من الرمل الخشن ذات قطر حبيبات متوسط 0.62 مم). استخدمت خمس قيم للتصرفات تتراوح من 0.5 لتر/ثانية إلى 15 لتر/ثانية ورقم فراود يتراوح ما بين 1.61 إلى 6.56. وكذلك خشونة نسبية (ارتفاع الشرائح إلى العمق الابتدائي للقفزة) يتراوح ما بين 0.5 إلى 2.0. استنتجت معدلات تربط ما بين خصائص النحر المتولد والعوامل المؤثرة، وقد وجد أن القيعان المثلثية تعتبر هي الأفضل من حيث تخفيض أبعاد النحر المتولد خلف القفزات الهيدروليكية.

### ABSTRACT:

This research work aims to study the effect of five different shapes; semi-circular, trapezoidal, spaced trapezoidal, triangular, spaced triangular corrugated beds on the corresponding scour downstream the hydraulic jump experimentally. Three different types of sand samples (fine sample with  $d_{50}=0.167\text{mm}$ , medium sample with  $d_{50}=0.365\text{mm}$  and coarse sample with  $d_{50}=0.62\text{mm}$ ) were used. Total of 285 experimental runs were performed using five values of discharge equal to 5, 8, 11, 13, and 15 lit./sec. and a wide range of Froude number ranging from 1.61 to 6.56. Six different relative roughness values equal to 0.5, 0.67, 0.8, 1.0, 1.33, and 2.0 were tested. From the analysis of data, it was found that the spaced triangular corrugated bed is the best for the reduction of hydraulic jump properties and consequently the corresponding scour dimensions.

### 1-INTRODUCTION:

Prediction of local scour holes developed downstream hydraulic structures plays an important role in their design. Excessive local scour can progressively undermine the foundation of the structure. The complete protection against scour is too expensive, so, the maximum scour depth and the upstream slope of the scour hole have to be predicted to minimize the risk of failure. Stilling basins are the popular and the designer's favorite choice for energy dissipation, because of the knowledge and experience acquired over the years.

Local scour is considered one of the important and complicated problems facing many of irrigation works, such as weirs, regulators, and dams, which are built crossing the flow of large alluvial channels and rivers. It is important to study the characteristics of scour, such as the maximum depth and length of scour that occurs downstream of irrigation structures to protect them from failure

Based on the mode of sediment transport by the approaching flow, Chabert and Engeldinger (1956) classified local scour into two categories,

namely, clear-water scour and live-bed scour, Fig. (1).

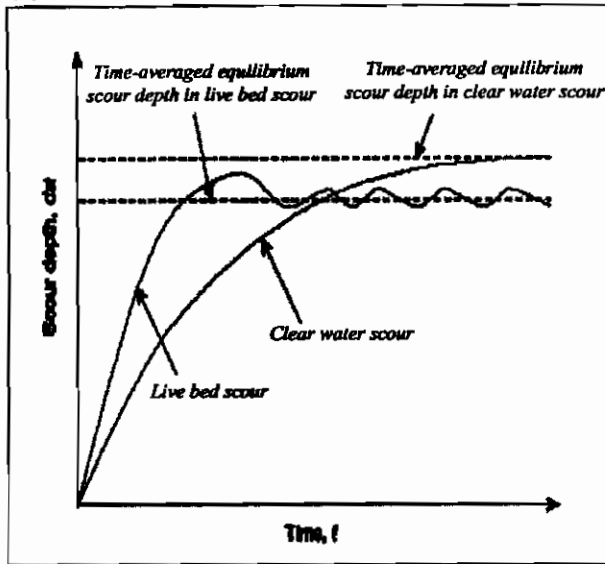


Fig. (1): Time development of clear-water and live-bed scour. (After Chabert and Engeldinger, 1956).

- Clear-water scour takes place in the absence of sediment transport into the scour hole.
- Live-bed scour occurs when the scour hole is continuously fed with sediment.

Chabert and Engeldinger (1956) found that the maximum clear-water scour depth is about 10% greater than the live-bed scour depth.

There are many formulas for scour following hydraulic jump in a stilling basin such as developed by Novak (1961), Catakli et al. (1973), Pillai et al. (1989), Rice et al. (1993), and Oliveto Giuseppe and Comuniello Victor (2009).

Scour downstream irrigation structures has been studied by many researchers such as Uymaz (1988), Baghdadi (1997), Hoffmans (1998) and El Abd (2002).

El Abd (2002) found that the scour hole depth increased with the increasing value of Froude number. For bigger values of stilling basin lengths, the values of  $(d/y_2)$  had small effect on the value of  $(d_s/y_2)$  for all values of Froude number.

Steady-flow experiments were carried out by Oliveto and Comuniello (2009) in long rectangular straight channel with 20-m long and 1-m wide using nearly uniform sandy beds and additional tests were performed with a special bed of lead spheres and for each run a submerged hydraulic jump formed. Tests were of long durations (of order of days) mainly to achieve conditions of

quasi-equilibrium. Empirical models are proposed to estimate the maximum scour depth and length. Artificial Neural Network (ANN) modeling using back-propagation learning technique was formulated to predict the maximum scour hole depth and length downstream hydraulic structure. Kheireldin (1999) used the ANN to predict the maximum depth of scour around bridge abutments. It was concluded that the ANN approach performed well for one set of data (305 runs) and its performance was not satisfactory for another set of data (66 runs).

Liriano and Day (2001) used the ANN to predict the scour hole depth at culvert outlet. They concluded that ANN could be used to predict the scour depth at the culvert outlet with a greater accuracy compared to the empirical scour formulae.

Negm et al. (2002) developed ANN model to predict maximum scour hole depth downstream of sudden expanding stilling basins.

Soliman (2007) developed a new ANN model to predict both length and depth of the scour hole downstream hydraulic structures.

It might be no experimental or theoretical investigations to illustrate the corresponding scour downstream hydraulic jumps over corrugated beds.

## 2- EXPERIMENTAL WORK

All experiments were conducted in a rectangular horizontal flume of 0.4 m wide, 0.4 m deep, and 12 m long, with 2 m long Perspex sides in the hydraulic laboratory of the Faculty of Engineering-El-Mansoura University. Corrugated wooden triangular, trapezoidal and semi-circular sheets, Plate (1), were installed on the flume bed in such away that the crests of corrugations were at the same level of upstream bed, Plate (2). The semi-circular and triangular shapes have a wave length (S) of 4.0 cm. The spaced trapezoidal corrugated bed (2 cm apart) has a wave length of 8.0 cm. The trapezoidal corrugated bed and the spaced triangular corrugated bed (2 cm apart) have a wave length of 6.0 cm, Fig. (2). All the corrugated bed models have an amplitude of 2.0 cm.

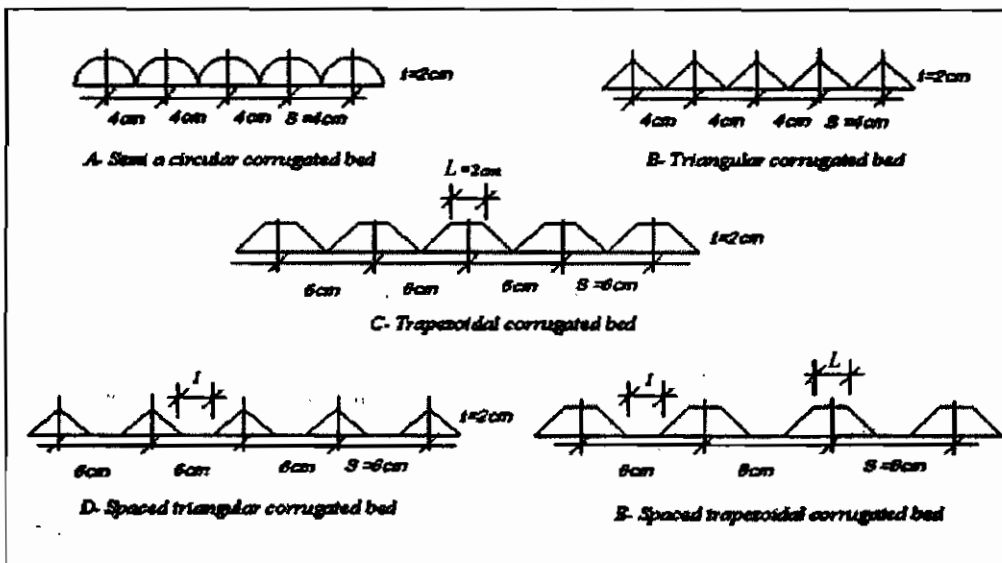
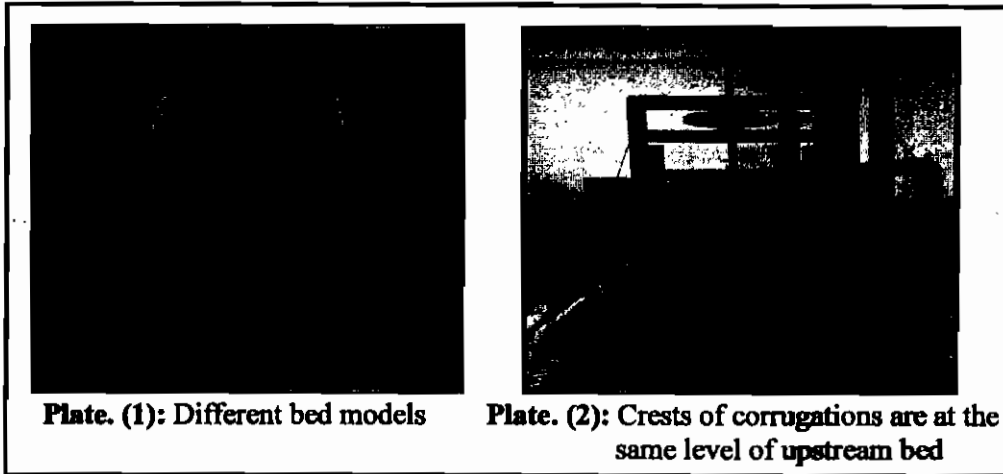


Fig. (2): Definition sketch shows different corrugated bed models.

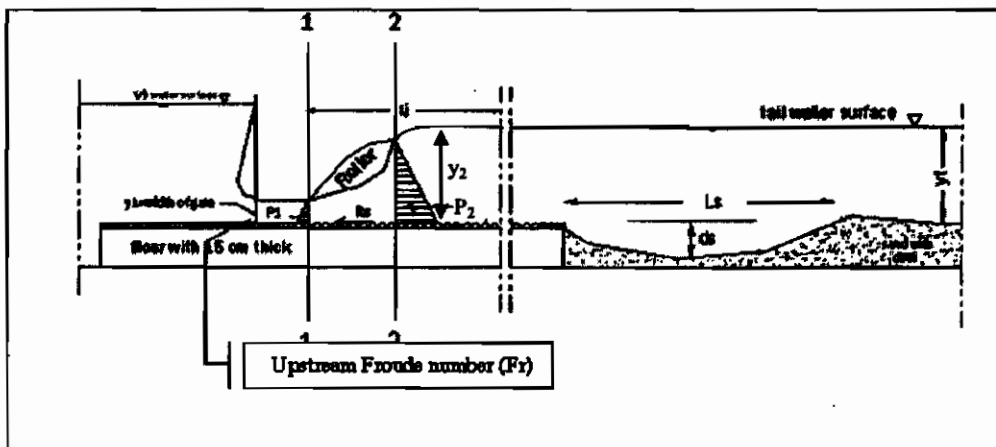


Fig. (3): Definition sketch shows scour hole downstream corrugated bed.

A streamlined lip sluice gate, Fig. (3), with screw wheel for lifting or lowering the gate was fixed on the middle of the approaching channel. This gate helps in suppressing the turbulence so that the flow issuing from the sluice gate is uniform and the *vena contracta* is avoided, consequently the slot width of the gate (height of gate opening) is equal to the initial depth of the jump ( $y_1$ ). A quarter of a pipe of about 8 cm (external radius) did this job.

A tail gate was used to control the tail water depth in the flume, and was adjusted so that the jumps were performed on the corrugated beds in all the experiments. Total of 285 experimental runs (15 for each model) were conducted throughout this study, and the convenient maximum discharge was found to be 15 lit. /sec. The water level was measured by a point gauge having an accuracy of 0.1mm.

The experimental work was carried out using three sand bed materials having different characteristics. Sieve analysis for sand samples is given in Fig. (4).

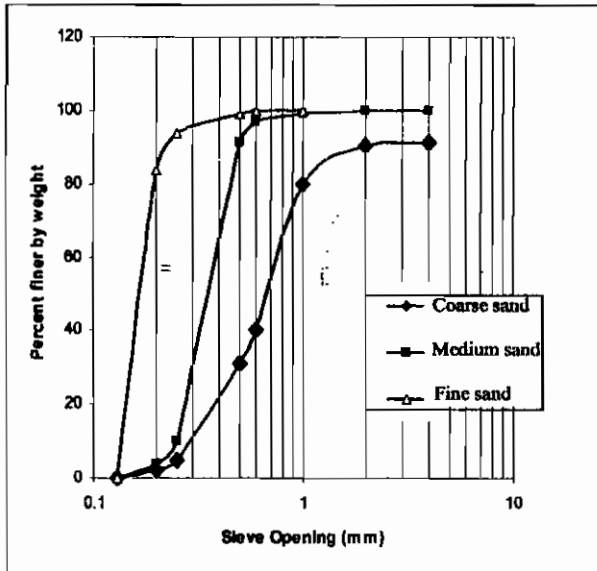


Fig. (4): Sieve analysis for sand samples

The characteristics of each sample are given in the following table (1).

Table (1): Properties of sand samples

Type	Sample No (1)	Sample No (2)	Sample No (3)
$d_{10}$	0.310 mm	0.260 mm	0.140 mm
$d_{50}$	0.620 mm	0.365 mm	0.167 mm
$\sigma$	1.6914	1.3263	1.1680
G	1.6917	1.3266	1.1683
$d_{65}$	0.8 mm	0.4 mm	0.18 mm
type	Coarse	Medium	Fine

### 3- ANALYSIS AND DISCUSSION

The effect of time on the scour hole depth and length for triangular bed is given in Fig. (5) and Fig. (6). It was noticed that the required time for settling the operation of scour was four hours. This time was nearly constant for all shapes of corrugations.

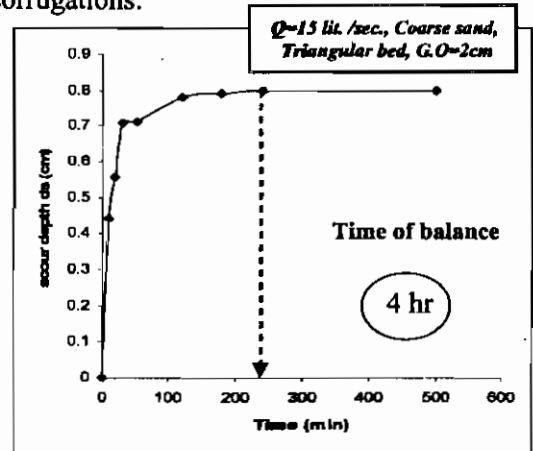


Fig. (5): Relationship between scour depth ( $d_s$ ) and time for triangular bed.

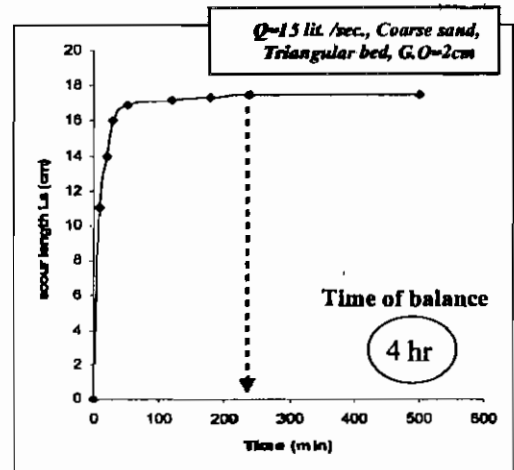


Fig. (6): Relationship between scour length ( $L_s$ ) and time for triangular bed.

It is assumed that the dependent variables; the depth of scour ( $d_s$ ) and the length of scour ( $L_s$ ), as shown in Fig. (3), are dependent on the following independent variables:

- initial depth of hydraulic jump ( $y_1$ );
- sequent depth of hydraulic jump ( $y_2$ );
- gravitational acceleration ( $g$ );
- mass density ( $\rho$ );
- dynamic viscosity ( $\mu$ );
- initial velocity of hydraulic jump ( $V_1$ );
- shape of corrugations ( $\zeta$ );
- median particle size ( $d_{50}$ );
- amplitude of corrugations ( $t$ );
- length of corrugated floor ( $L_f$ );
- time taking for stability of scour hole ( $T$ );
- shear velocity at bed surface of corrugations ( $V^*$ ); and
- length of corrugation sample ( $S$ ).

then, using  $\pi$  theorem:

$$\frac{d_s}{y_1} = f_1 \left( \frac{y_2}{y_1}, Fr, Re, \zeta, \frac{t}{y_1}, \frac{d_{50}}{y_1}, \frac{L_f}{y_1}, \frac{TV_1 S}{y_1}, \frac{V_1}{V^*} \right) \quad (1)$$

and;

$$\frac{L_s}{y_1} = f_2 \left( \frac{y_2}{y_1}, Fr, Re, \zeta, \frac{t}{y_1}, \frac{d_{50}}{y_1}, \frac{d_s}{y_1}, \frac{L_f}{y_1}, \frac{TV_1 S}{y_1}, \frac{V_1}{V^*} \right) \quad (2)$$

The time of balance for the scour depth and the scour length was found to be four hours for all runs, then the term  $(TV_1/y_1)$  could be neglected.

As the channel width is 40 cm and the initial water depth of hydraulic jump ( $y_1$ ) was found to vary between 1cm and 4cm from the experimental work, then the value of  $(b/y_1)$  ranges from 10 to 40, this means that the channel could be assumed to be wide, based on that, ( $y_1$ ) is equal to the hydraulic radius. The experimental work exhibited value of Reynolds number varies between 32500 and 37750, then viscosity of water has no effect and Reynolds number could be neglected.

### 3.1. Scour Hole Depth

Figs. (7), (8) and (9) give the relationship between the scour depth ( $d_s/y_1$ ) and the upstream Froude number for coarse, medium and fine sand samples respectively.

It may be concluded from these figures:

- the scour depth at semi-circular, trapezoidal, triangular, spaced trapezoidal and spaced triangular corrugated beds decreases by a range from (23.75% to 34.74%), (25.61% to 35.68%), (31.51% to 37.67%), (39.82% to 50.3515%) and (41.67% to 56.211%) respectively from the scour depth of smooth bed;
- the spaced triangular corrugated bed (2cm apart) could be considered the best corrugated bed for the reduction of the scour hole depth for all sand types;
- semi-circular, trapezoidal and triangular corrugated beds have nearly the same effect on the scour depth. Consequently the study has concentrated on the triangular bed; and
- for small values of geometric mean size of sand particles ( $d_{50}$ ), the percent of reduction in the depth of scour for the spaced corrugated beds (trapezoidal and triangular) increases more than that given by other shapes.

For coarse sand

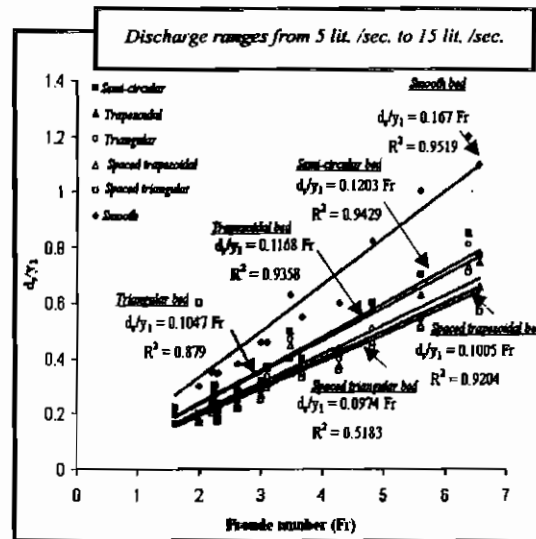


Fig. (7): Relationship between ( $d_s/y_1$ ) and the upstream Froude number ( $Fr$ ) for different corrugated beds.

For Medium sand

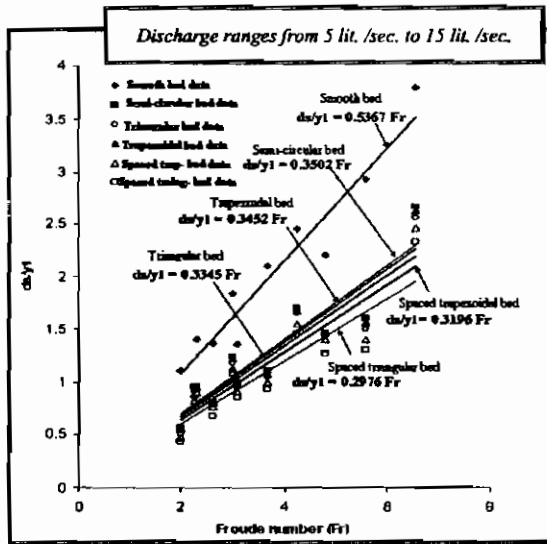


Fig. (8): Relationship between ( $d_s/y_1$ ) and the upstream Froude number ( $Fr$ ) for different corrugated beds.

For fine sand

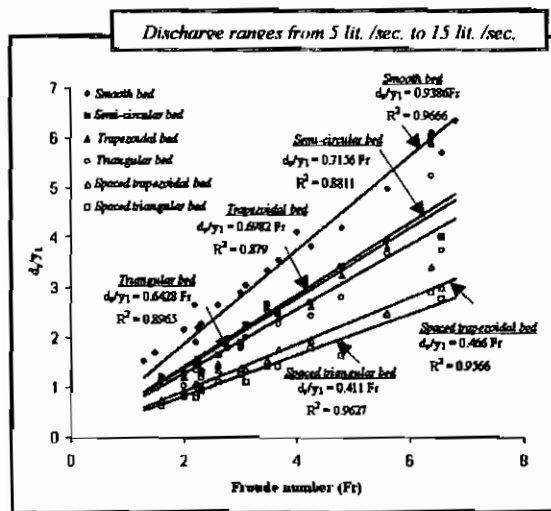


Fig. (9): Relationship between ( $d_s/y_1$ ) and the upstream Froude number ( $Fr$ ) for different corrugated beds.

3.2. Scour Hole Length

Figs. (10), (11) and (12) give the relationship between the scour depth ( $L_s/y_1$ ) and the upstream Froude number for coarse, medium and fine sand samples respectively.

It may be noticed from these figures:

- the scour length at semi-circular, trapezoidal, triangular, spaced trapezoidal and spaced triangular corrugated beds decreases by a range from (17.78% to 23.11%), (22.66% to 24.22%), (24% to 28.36%), (27.54% to 32.9%) and (31.33% to 34.32%) respectively from the scour length of smooth bed;
- the spaced triangular corrugated bed (2cm apart) could be considered the best corrugated bed for the minimization of the scour hole length for all sand types; and
- the reduction range of scour hole depth is more than the reduction range of scour length by about 9% for coarse sand, 13.22% for medium sand and 21.9% for fine sand for the spaced triangular bed.

For coarse sand

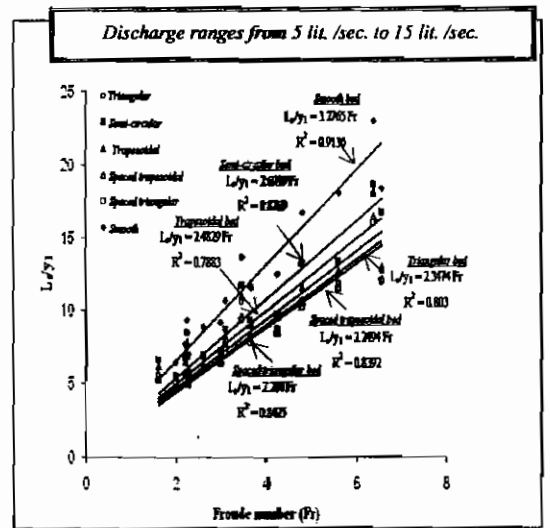


Fig. (10): Relationship between ( $L_s/y_1$ ) and the upstream Froude number ( $Fr$ ) for different corrugated beds.

For Medium sand

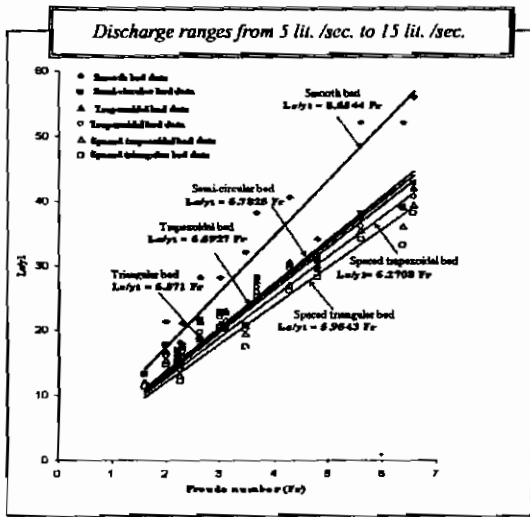


Fig. (11): Relationship between  $(L_s/y_1)$  and the upstream Froude number  $(Fr)$  for different corrugated beds.

For fine sand

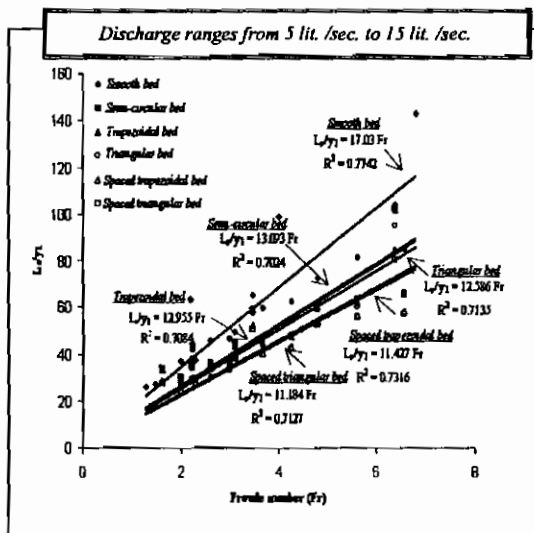


Fig. (12): Relationship between  $(L_w/y_1)$  and the upstream Froude number  $(Fr)$  for different corrugated beds.

As the spaced triangular bed is considered the best for the reduction of scour hole depth and length, it is important to study each of the dimensionless parameters affect on the scour hole depth and length for this bed models.

The effect of  $(S/y_1)$  and  $(t/y_1)$  on the scour hole properties, as shown in the present study and previous works (El-Gamal (2010)), could be neglected.

Fig. (13) shows the relationship between  $(V_1/V^*)$  and the upstream Froude number for different corrugated beds.

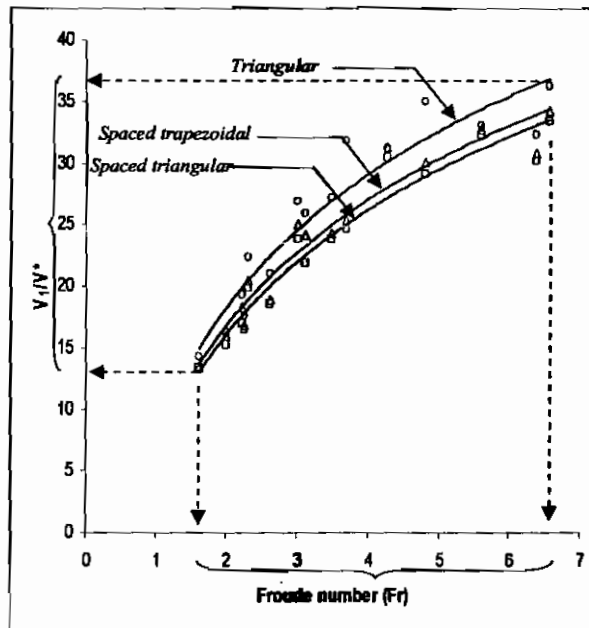


Fig. (13): Relationship between  $(V_1/V^*)$  and the upstream Froude number  $(Fr)$  for triangular, spaced trapezoidal and spaced triangular corrugated beds (discharge ranges from 8 lit./sec. to 15 lit./sec.)

From this figure, it was found that:

- the values of  $(V_1/V^*)$  for spaced triangular bed are greater than the corresponding values for spaced trapezoidal and triangular beds;
- for spaced trapezoidal corrugated bed, the values of  $(V_1/V^*)$  are greater than the corresponding values for triangular bed;

- the shape of spaced corrugations do not have a great effect on the relationship between  $(V_1/V^*)$  and Froude number;
- it is seen from the previous figure, the values of  $(V_1/V^*)$  ranges from 13.33 to 36.22 for Froude number varied between 1.61 and 6.56; and
- at this range of Froude number, the value of shear velocity  $(V^*)$  ranges from 0.052 m/sec to 0.075 m/sec, and consequently, the effect of shear velocity on the scour depth and length for different bed models might be neglected due to this small range.

The relationship between  $(V_1/V^*)$  and upstream Froude number is given by:

For triangular corrugated bed,

$$\frac{V_1}{V^*} = 15.64 \ln(Fr) + 7.399 \quad (R^2=0.9) \quad (3)$$

For spaced trapezoidal corrugated bed,

$$\frac{V_1}{V^*} = 14.77 \ln(Fr) + 6.558 \quad (R^2=0.94) \quad (4)$$

For spaced triangular corrugated bed,

$$\frac{V_1}{V^*} = 14.63 \ln(Fr) + 5.93 \quad (R^2=0.95) \quad (5)$$

Figs. (14) through (19) illustrate the effect of changing  $(V_1/V^*)$  on the characteristics of scour  $(d_s)$  and  $(L_s)$  for triangular, spaced trapezoidal and spaced triangular corrugated beds at a discharge ranges from 8 lit. /sec. to 15 lit. /sec.

It was concluded that:

- at small values of  $(V_1/V^*)$ , minimum relative values of both the scour depth and length occur, and vice versa;
- the value of  $(L_s/y_1)$  ranges from about 30 to 60, for a range of Froude numbers from 1.61 to 6.56. for different corrugated beds;
- the value of  $(d_s/y_1)$  at Froude number from 1.61 to 6.56, ranges from 0.6 to 2.6 for different corrugated beds; and
- the best relationships between  $(L_s/y_1)$  and  $(V_1/V^*)$  are polynomial functions of fourth degree.

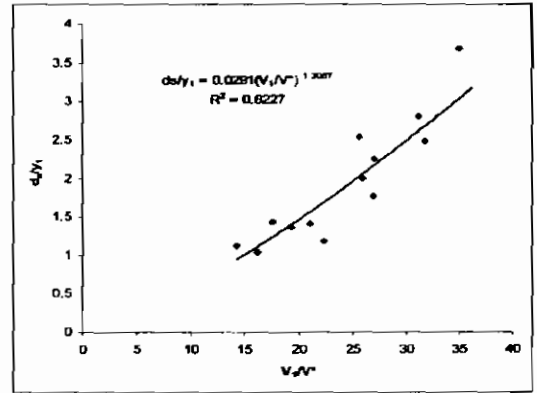


Fig. (14): Relationship between  $(d_s/y_1)$  and  $(V_1/V^*)$  for triangular corrugated bed (discharge ranges from 8 lit. /sec. to 15 lit. /sec.)

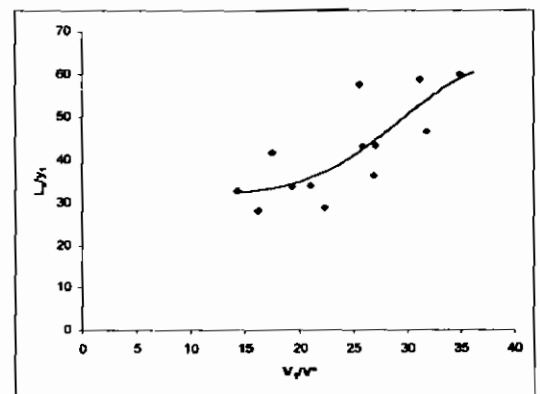


Fig. (15): Relationship between  $(L_s/y_1)$  and  $(V_1/V^*)$  for triangular corrugated bed (discharge ranges from 8 lit. /sec. to 15 lit. /sec.)

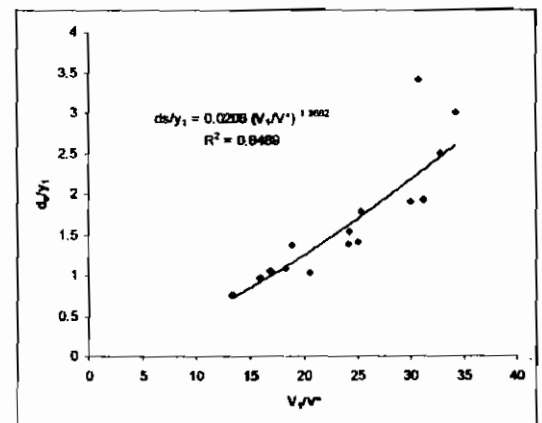
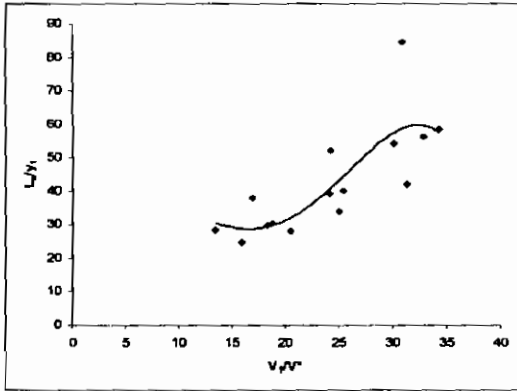
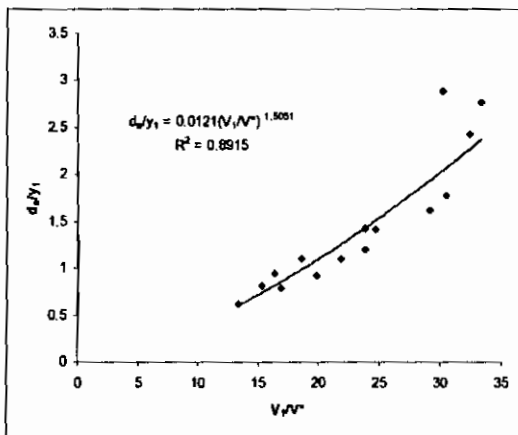


Fig. (16): Relationship between  $(d_s/y_1)$  and  $(V_1/V^*)$  for spaced trapezoidal corrugated bed (discharge ranges from 8 lit. /sec. to 15 lit. /sec.)





**Fig. (17):** Relationship between  $(L_s/y_1)$  and  $(V_1/V^*)$  for spaced trapezoidal corrugated bed (discharge ranges from 8 lit. /sec. to 15 lit. /sec.)



**Fig. (18):** Relationship between  $(d_s/y_1)$  and  $(V_1/V^*)$  for spaced triangular corrugated bed (discharge ranges from 8 lit. /sec. to 15 lit. /sec.)

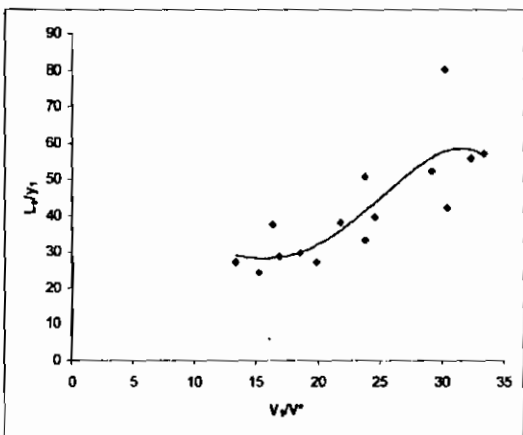


**Fig. (19):** Relationship between  $(L_s/y_1)$  and  $(V_1/V^*)$  for spaced triangular corrugated bed (discharge ranges from 8 lit. /sec. to 15 lit. /sec.)

**3.3. Samples of contour maps**

Figs. (20) through (24) give the effect of bed material and the shape of corrugated bed on the scour contour maps. It was appeared from these figures that the maximum scour hole depth was at the center line of the channel width and the effect of the channel boundaries on the scour contours is very small and does not appear in contour maps.

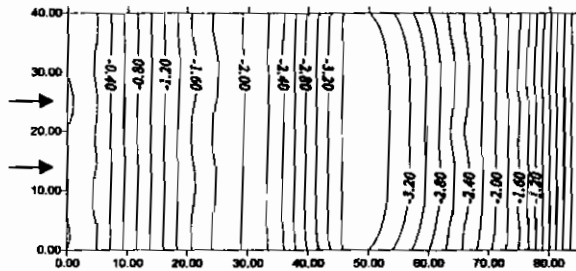


**Fig. (20):** Contour map of scour hole at  $(Q=15$  lit. /sec.,  $y_1=2.5$ cm, spaced trapezoidal bed (2cm apart), fine sand)

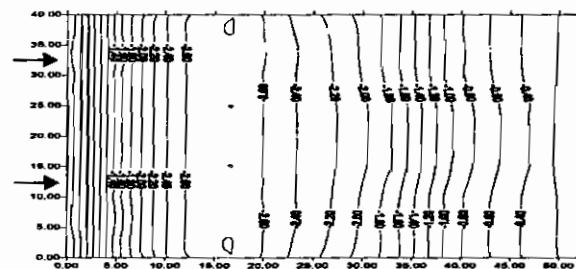


**Fig. (21):** Contour map of scour hole at  $(Q=15$  lit. /sec.,  $y_1=2.5$ cm, spaced trapezoidal bed (2cm apart), medium sand)

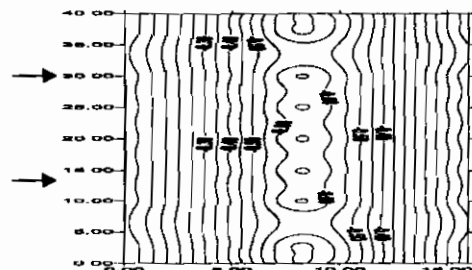


**Fig. (22):** Contour map of scour hole at  $(Q=15$  lit. /sec.,  $y_1=2.5$ cm, spaced trapezoidal bed (2cm apart), coarse sand)

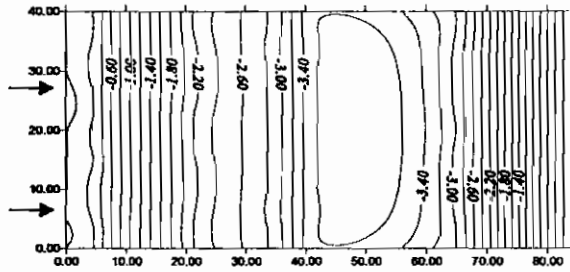


Fig. (23): Contour map of scour hole at (Q=15 lit./sec.,  $y_1=2.0$ cm, spaced triangular bed (2cm apart), fine sand)

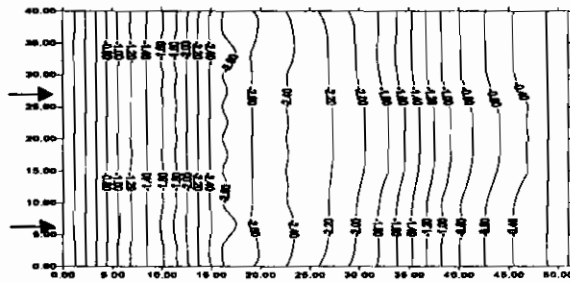


Fig. (24): Contour map of scour hole at (Q=15 lit./sec.,  $y_1=2.5$ cm, spaced triangular bed (2cm apart), medium sand)

### 3.4. Empirical relationships for scour hole depth and length for all bed models for this study

#### ☒ Smooth bed

$$\bullet \frac{ds}{y_1} = 0.05F_r^{3.24} \left( \frac{d_{50}}{y_1} \right)^{-0.94} \left( \frac{y_2}{y_1} \right)^{-1.59} \quad (R^2=0.71) \quad (6)$$

$$\bullet \frac{L_s}{y_1} = 1.877F_r^{3.27} \left( \frac{d_{50}}{y_1} \right)^{-0.73} \left( \frac{y_2}{y_1} \right)^{-1.82} \quad (R^2=0.63) \quad (7)$$

#### ☒ Semi-circular bed

$$\bullet \frac{ds}{y_1} = 0.0193F_r^{5.26} \left( \frac{d_{50}}{y_1} \right)^{-1.21} \left( \frac{y_2}{y_1} \right)^{-3.43} \quad (R^2=0.86) \quad (8)$$

$$\bullet \frac{L_s}{y_1} = 0.08F_r^{4.94} \left( \frac{d_{50}}{y_1} \right)^{-1.68} \left( \frac{y_2}{y_1} \right)^{-2.68} \quad (R^2=0.66) \quad (9)$$

#### ☒ Trapezoidal bed

$$\bullet \frac{ds}{y_1} = 0.0139F_r^{4.85} \left( \frac{d_{50}}{y_1} \right)^{-1.22} \left( \frac{y_2}{y_1} \right)^{-2.89} \quad (R^2=0.86) \quad (10)$$

$$\bullet \frac{L_s}{y_1} = 0.505F_r^{4.88} \left( \frac{d_{50}}{y_1} \right)^{-1.15} \left( \frac{y_2}{y_1} \right)^{-3.21} \quad (R^2=0.874) \quad (11)$$

#### ☒ Triangular bed

$$\bullet \frac{ds}{y_1} = 0.0464F_r^{2.79} \left( \frac{d_{50}}{y_1} \right)^{-1.15} \left( \frac{y_2}{y_1} \right)^{-0.84} \quad (R^2=0.81) \quad (12)$$

$$\bullet \frac{L_s}{y_1} = 1.3316F_r^{2.53} \left( \frac{d_{50}}{y_1} \right)^{-1.15} \left( \frac{y_2}{y_1} \right)^{-0.82} \quad (R^2=0.81) \quad (13)$$

#### ☒ Spaced trapezoidal bed (2cm apart)

$$\bullet \frac{ds}{y_1} = 0.0162F_r^{3.41} \left( \frac{d_{50}}{y_1} \right)^{-1.03} \left( \frac{y_2}{y_1} \right)^{-1.66} \quad (R^2=0.80) \quad (14)$$

$$\bullet \frac{L_s}{y_1} = 0.375F_r^{4.01} \left( \frac{d_{50}}{y_1} \right)^{-1.12} \left( \frac{y_2}{y_1} \right)^{-2.35} \quad (R^2=0.85) \quad (15)$$

#### ☒ Spaced triangular bed (2cm apart)

$$\bullet \frac{ds}{y_1} = 0.01617F_r^{2.81} \left( \frac{d_{50}}{y_1} \right)^{-0.98} \left( \frac{y_2}{y_1} \right)^{-1.09} \quad (R^2=0.80) \quad (16)$$

$$\bullet \frac{L_s}{y_1} = 0.3373F_r^{3.77} \left( \frac{d_{50}}{y_1} \right)^{-1.11} \left( \frac{y_2}{y_1} \right)^{-2.1} \quad (R^2=0.86) \quad (17)$$

In which;

$y_b, y_2, d_s$  and  $L_s$  in cm,  $d_{50}$  in mm.

#### 4. SUMMARY AND CONCLUSIONS

For the range of the experimental data of the present study it is concluded that:

- Three different corrugated sheets (semi-circular, trapezoidal and triangular) have been used to study the effect of corrugations on the characteristics of scour downstream free hydraulic jumps using three different sand samples.
- The time of balance for scour hole depth and length was found to be about four hours for all sand types.
- From the experimental work it was noticed that, the depth and length of the scour hole reached to about 85%, 79% respectively from its total value after one hour.
- Many parameters affect the scour properties but, only some of these parameters such as Froude number, ratio between conjugate depths and the geometric mean size of sand particles are used to express these properties.
- Semi-circular, trapezoidal and triangular corrugated beds have nearly the same effect on the scour hole properties for all sand types.
- There are a wide range between the effect of spaced trapezoidal or spaced triangular corrugated beds and the other beds on the scour characteristics.
- Spaced triangular bed could be considered the best corrugated bed for the reduction of scour hole depth and length.
- Empirical equations were deduced to express the relationships between both the scour depth and length and the main effective parameters for a range of Froude number from 1.61 to 6.56.

#### ACKNOWLEDGMENTS:

This research paper is a part of the fourth author M.Sc thesis and the experimental work was conducted in the hydraulic laboratory of the Faculty of Engineering -El-Mansoura University.

#### REFERENCES

- [1] Baghdadi, K.H. (1997). " Local Scour downstream Drop Structure", Alexandria Engineering Journal, Vol. 36, No. 2.
- [2] Cataki, O. et al. (1973). " A study of Scour at the End of Stilling Basin and Use of Horizontal Beams as Energy Dissipators", 11<sup>th</sup> Congres of Large Dams, Madrid.
- [3] El Abd, S.M. (2002) . " Effect of Using Stilling Basins on Local Scour Downstream Irrigation Structures", M. Sc. Thesis, Irrigation and Hydraulic Dept. El-Mansoura University, Egypt.
- [4] El-Gamal, M.I. (2010). "Hydraulic Jumps on Corrugated Beds and the Corresponding downstream Scour", M.Sc thesis (in progress), Irrigation and Hydraulic Department, El-Mansoura University.
- [5] Hoffmans, G.J.C.M. (1998). " Jet Scour in Equilibrium Phase", Journal of Hydraulic Engineering, ASCE, Vol. 124, No. HY 4, pp. 430-437.
- [6] Kheireldin, K.A. (1999). " Neural Network Modeling for Clear Water Scour around Bridge Abutments", Journal of Water Science, National Water Research Center, MWRI, El-Qanatir, Egypt, Vol. 25, No. 4, pp. 42-51.
- [7] Liriano, S.L., and Day, R.A. (2001). " Prediction of Scour Depth at Culvert Outlet Using Neural Networks", Journal of Hydro-informatics, Iran, Vol. 3, No. 4.
- [8] Negm, A.M, et al. (2002). " Prediction of Hydraulic Design Parameters of Expanding Stilling Basins, Using Artificial Neural Networks ", Egyptian Journal of Engineering Science and Technology, Zagazig University, Vol. 6, No. 1, pp. 1-24.
- [9] Novak, P.J. (1961). " Influence of Bed Load Passage on Scour and Turbulence downstream of Stilling Basin", 9<sup>th</sup> Congress, IAHR, Dubrovnik, Croatia.
- [10] Oliveto ,G., and Victor, C. (2009). " Local Scour downstream of Positive-Step Stilling Basins", Journal of Hydraulic

Engineering, ASCE, Vol.135, No 10, pp. 846-851.

**NOTATION:**

The following symbols are used in this paper:

- [11] Pillai, N.N., et al. (1989). "Hydraulic Jump Type Stilling Basin for Low Froude Numbers", Journal of Hydraulic Engineering, ASCE, Vol. 115, No. HY 7, pp. 989-994.
- [12] Rice, C.E., and Kadavy, K.C. (1993). "Protection against Scour at SAF Stilling Basins", Journal of Hydraulic Engineering, ASCE, Vol. 119, No. HY 1, pp. 133-139.
- [13] Soliman, M. (2007). "Artificial Neural Network Prediction of Maximum Scour Hole downstream Hydraulic Structures", National Water Research Center, Egypt.
- [14] Uymaz, A. (1988). "The Investigation of the Scours Originating when Water Passes Simultaneously over and under Vertical Gates", Journal of Hydraulic Engineering, ASCE, Vol. 114, No. HY 7, pp.811-816.

$b$  = channel width;  
 $d_s$  = maximum scour depth;  
 $F_r$  = upstream Froude number;  
 $G$  = gradation coefficient;  
 $G.O$  = gate opening;  
 $g$  = acceleration of gravity;  
 $I$  = clearance distance between corrugated sheets;  
 $L$  = small trapezoidal base;  
 $L_f$  = length of floor;  
 $L_s$  = maximum scour length;  
 $S$  = wave length between two corrugated sheets;  
 $T$  = balancing scour time;  
 $t$  = amplitude of the corrugations;  
 $V_1$  = flow velocity upstream the jump;  
 $V^*$  = shear velocity;  
 $y_1$  = initial depth of hydraulic jump;  
 $y_2$  = sequent depth of hydraulic jump over corrugated bed;  
 $\zeta$  = index for the shape of corrugations;  
 $\mu$  = dynamic viscosity of water;  
 $\rho$  = density of water; and  
 $\sigma$  = standard deviation of sand particles.